

## **SYNTHESIS AND CHARACTERIZATION OF RPET/ORGANO-MONTMORILLONITE NANOCOMPOSITES**

**Blessie A. Basilia<sup>1</sup>, Herman D. Mendoza, Dr. Eng.<sup>2</sup>  
and Leonorina G. Cada, Ph.D.<sup>3</sup>**

<sup>1</sup>PhD MSE Program, DMME, College of Engineering  
University of the Philippines, Diliman, Quezon City

<sup>2</sup>National Engineering Center, University of the Philippines,  
Diliman, Quezon City

<sup>3</sup>INTEL, Philippines, Cavite

### **ABSTRACT**

*Recycled polyethylene terephthalate (RPET)/organo-montmorillonite nanocomposites were synthesized by direct melt intercalation method. The effect of this processing technique in the nanomorphology, thermal stability and mechanical behavior of the intercalated products were characterized by X-ray diffraction (XRD), high resolution transmission electron microscopy (HRTEM), small angle x-ray scattering (SAXS), differential scanning calorimetry (DSC), thermogravimetric analysis (TGA) and mechanical analysis. The difference of using recycled PET (RPET) vis-à-vis virgin PET (VPET) as matrix in the polymer nanocomposites, using synthesized Philippine organo-montmorillonite or commercial organoclay as the layered-silicate, was evaluated. Results showed that direct melt intercalation by twin-screw extrusion method gave generally exfoliated structures especially at <5% clay loading, based on powder XRD patterns. SAXS patterns and HRTEM micrographs revealed laminated structures at the basal (001) reflections resulting to a d-spacing of 14nm in localized areas not observed by powder diffraction. Higher levels of orientation of the layered silicates were obtained with commercial organoclay compared with the synthesized clay. Thermal degradation has been decreased and tensile strength increased with the increase in clay loading. RPET resin was intercalated in a similar manner with VPET in the layered silicates of Philippine organo-montmorillonite.*

### **I. Introduction**

Traditionally, reinforcing agents such as fibers and mineral fillers have been added to thermoplastics and thermosets to form conventional composites. The recent advances in synthetic techniques to characterize materials on an atomic scale have led to the interest in the development of nanometer-size materials. Since nanometer-size grains (10-100Å) in at least one dimension have dramatically increased surface area, the chemistry of these nanosized materials is altered compared to conventional materials [1,2]. Nanocomposites are now considered as one of the important technologies in plastics application.

Montmorillonite is an essential raw material for the synthesis of polymer nanocomposites. Various surface treatment chemistries and technologies can be developed to compatibilize these nanoclays with a wide variety of matrix polymers [3,4]. By exchanging the exchangeable ions of montmorillonite with various organic cations, such as the quaternary alkylammonium cations, they can be modified to become hydrophobic and oleophilic for advanced industrial applications.

Various methods had been developed to prepare polymer layered silicate nanocomposites (PLSN) [5]. One method is by direct melt intercalation technique [4, 6, 7]. It involves the diffusion of the molecules from the bulk polymer melt into the van der Waals galleries between the silicate layers by hot blending or mixing. The polymer chains can undergo center of mass transport in between the clay layers. The radius of gyration of the polymer is roughly an order of magnitude greater than the interlamellar spacing of the clay. The proposed driving force for this mechanism is the important enthalpic contribution of the polymer/organoclay interactions during the blending/mixing [4].

The polymer matrix, polyethylene terephthalate (PET), is a widely accepted and very popular packaging material particularly for food because of its good performance, relatively cheap cost and easy reproducibility. Over five (5) million tones of PET are processed worldwide to make bottles and the trend is growing. There is now a clear and increasing concern over the recycling of PET. As a result, a European plastics recycling company called EREMA has developed a recycling process that is able to withdraw chemical impurities and toxicants from processed PET in a very highly effective manner [8]. Recycling generally results in a degraded recycled structure when compared to the initial molecule.

This research aims to synthesize RPET/organo-montmorillonite nanocomposites by direct melt intercalation technique. It will also investigate how the interaction of the three-layered silicate (montmorillonite) influences the structural properties, thermal stability and mechanical properties of a recycled resin compared with virgin resin, and create a knowledge base for further application of the nanocomposites.

## **II. Materials and Methods**

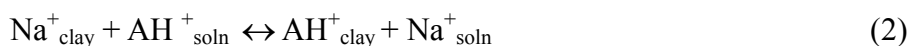
### *2.1 Raw Materials and activation techniques*

Two (2) types of PET resins were used: a) recycled polyethylene terephthalate (RPET) - supplied by EREMA Plastics Recycling Systems of Austria, and b) virgin polyethylene terephthalate (VPET) - supplied by Coca-Cola Bottlers Philippines, Inc., (CCBPI).

The organo-montmorillonite or organoclay (OMMT) was processed by first treating natural calcium-montmorillonite (Ca-MMT), from the deposit in Legaspi, Albay (Philippines), with sodium carbonate ( $\text{Na}_2\text{CO}_3$ ) to produce sodium-montmorillonite (Na-MMT). The ion-exchange reaction involved is given by:



Then organic activation was conducted by adding dialkyl dimethyl ammonium chloride ( $\text{C}_{22}\text{H}_{48}\text{ClN}$ ), manufactured by Fluka (Switzerland), to modify the surface of the clay making it hydrophobic and oleophilic [9-11]. The cation exchange reaction involved is:



This exchange process has been described by Theng (12) as a reaction that applies when all the amine cations are completely, or nearly completely replaced with the exchangeable sodium ions of the clay, where A and  $\text{AH}^+$  refer to the free amine and the amine cation (alkylammonium), respectively.

A commercial organo-modified montmorillonite (FLUKA) from Switzerland was used as reference. Experiments were conducted using this clay in parallel conditions with the Philippine organoclay (PHIL).

## 2.2 Direct Melt Intercalation Technique

Melt intercalation was conducted in a Brabender counter-rotating twin screw extruder DSE 25 with a barrel diameter of 25 mm and processing length of 48D. The average temperature of the extrusion processing zone was  $270^\circ\text{C}$  while the temperature of the die was  $260^\circ\text{C}$ . The screw speed used was 81 rpm. The extrudate was quenched in water and pelletized using a Brabender pelletizer (Model:881204). Using this process, the RPET resin was intercalated in the layered silicates of organoclay (PHIL) at parallel conditions with the reference samples (VPET and FLUKA) at the following clay loadings: 1, 3, 5 and 10 wt%.

## 2.3 Characterization Techniques

*X-ray Diffraction (XRD)*: XRD patterns were obtained from Rigaku 2000 using CuK- $\alpha$  target set at 36kV and 20mA. The divergence slit used was  $1^\circ$ , scattering slit:  $1^\circ$ , receiving slit: 0.3 mm, scan rate:  $1^\circ/\text{min}$ , and step size:  $0.05^\circ$ .

*Small Angle X-ray Scattering (SAXS)*: Temperature-variable SAXS measurement was carried out using a custom-built apparatus. A Rigaku UltraX18 [50 kV (290 mA)] rotating-anode X-ray generator, was mounted on the custom set-up.

*Differential Scanning Calorimetry (DSC)*: The thermal properties of the samples were determined using a DSC 22 System, Seiko Instruments, Inc., Japan. The heating rate used was 10°/min and the temperature range was 30- 300°C at nitrogen atmosphere. The percent crystallinity [13] was determined using the following equation (3).

$$\%C \text{ (Crystallinity)} = [(\Delta H_m - \Delta H_c) / \Delta H_m^0] \bullet 100\% \quad (3)$$

where  $\Delta H_m$  is the heat of fusion, and  $\Delta H_c$  is the heat of cold crystallization in J/g. The term  $\Delta H_m^0$  is a reference value and represents the heat of melting of the polymer which is 100% crystalline.

*Transmission Electron Microscope (TEM)*: The nanocomposite specimens were analyzed using the JEOL JEM-1200EXII at 120 kV. Ultrathin samples were prepared using an ultramicrotome with a diamond knife made by Reichert-Nissei Ultracuts, MEIJI, EMZ Meij Techno Co. Ltd., Leica. The thickness of the final sample was about 30 nm. These samples were further examined using a HRTEM of JEOL JEM – 3010 at 300kV.

*Thermogravimetric Analysis (TGA)*: This analysis was conducted using a Rigaku Thermo Plus TG 8120 at a temperature range of 25 - 650° C and heating rate of 10°/min at air flow conditions.

*Mechanical Analysis*: The tensile strength and modulus were determined using the Instron Model 8872, in accordance with ASTM D 638-91 [14], and using a crosshead speed of 25mm/min and a gauge length of 50 mm. The values reported were taken from the average of five (5) measurements per sample at room temperature.

### III. Results and Discussions

#### 3.1 Structural effect in the sodium and organic-activation of montmorillonites

The natural Ca-MMT was converted to Na-MMT by ion exchange reaction when  $\text{Na}_2\text{CO}_3$  solution was added. By ion-exchange reaction, the  $\text{Ca}^{2+}$  of Ca-MMT was replaced by  $\text{Na}^+$  of  $\text{NaCO}_3$  in the interlayer space resulting to a change in basal (001) spacing from 1.54nm to 1.41nm (Figure 1). Furthermore, there has been an expansion of the interlayer space after organic activation with quaternary alkylammonium salt of Na-MMT, from 1.41nm to a multi-layered structure giving d-spacings: 1.27nm, 2.07nm and 3.66nm. The orientation and arrangement of interlayer organic molecules were deduced from basal spacing measurements [15, 16]. In this case, paraffinic structures were obtained upon organic activation. This indicates that there was a crowding of the hydrocarbon chains causing it to overlap and tilt perpendicular to the silicate surface. The presence of the alkyl ammonium cations lowers the surface energy of montmorillonite and improves the wetting characteristics with the polymer matrix [17, 18].

Ca-MMT showed randomly arranged flaky particles with curled edges of various sizes in the FESEM micrograph (Figure 2). Upon sodium activation, these particles turned into fluffy masses of irregular shape as shown in the FESEM micrograph of Na-MMT. Organic activation to produce OMMT showed a random stacking of thin plate-like particles in the TEM micrograph. These lamellar aggregate structures were expanded to various degrees in the adjacent layers exposing it for intercalation with polymers.

FT-infrared spectroscopy further characterized the adsorption of the quaternary alkylammonium salts by montmorillonite (Figure 3). The bands that described the interaction of the DADM alkylammonium cations with montmorillonite are given by the C-H and N-H stretchings at  $2850\text{ cm}^{-1}$  and  $2916\text{ cm}^{-1}$ , respectively. The C-H bands found in the OMMT also appeared in the FTIR spectra of both VPET and RPET resins, which indicate that the OMMT may have an affinity or miscibility with the polymer during melt intercalation

### 3.2 *Structural and thermal properties of PET resins*

The XRD spectra of RPET and VPET show identical patterns wherein both exhibited crystalline structures (Figure 4). The similarities of the two resins indicate that EREMA [8] had successfully processed a recycled resin comparable with the virgin resin. The recycling process was able to withdraw chemical impurities and toxicants from the processed PET in a very highly effective manner.

The thermal behavior of both RPET and VPET resins are shown in the DSC patterns during the first and second heating (Figure 5). RPET showed insignificant change in both heating stages (a and b) while VPET showed a cold crystallization stage in the second heating (d), which did not appear in the first heating (c). RPET has a higher glass transition temperature ( $T_g$ ), but lower melting temperature ( $T_m$ ) compared with VPET, based on the 2<sup>nd</sup> heating (Table 1). VPET became amorphous after quenching with liquid nitrogen.

Cold crystallization exothermic peak may or may not be observed during the DSC experiment because it is dependent upon the sample's given thermal history [19, 20]. The quenching or rapid cooling from the melt did not give the VPET resin the time to develop a significant crystalline component. However, RPET remained to be semi-crystalline with 20.4% crystallinity after quenching with liquid nitrogen. The level of crystallinity is a key property in PET because it is related to brittleness, toughness, stiffness or modulus, barrier resistance and optical clarity of the product [13].

### 3.3 *Effect of hybrid formation by direct melt intercalation*

#### 3.3.1 *Nanostructures of PET-organoclay nanocomposites*

Hybrid formation of nanocomposites involves the break-up and dispersion of the agglomerated stacks of montmorillonite sheets followed by the swelling of the gallery spacing between the sheets upon intercalation of the polymer [21]. Two terms

(intercalated and exfoliated) are used to describe the two general classes of nanomorphology that can be prepared by direct melt intercalation method. Intercalated structures are self-assembled, well-ordered multilayered structures where the extended polymer chains are inserted into the gallery space between parallel individual silicate layers separated by 2-3 nm [1, 22]. The exfoliated (or delaminated) structures result when the individual silicate layers are no longer close enough to interact with the adjacent layers' gallery cations. In this case, the interlayer spacing can be on the order of the radius of gyration of the polymer; therefore, the silicate layers may be considered to be well-dispersed in the organic polymer. Both of these hybrid structures can also co-exist in the polymer matrix. This mixed nanomorphology is very common for composites based on layered silicates [1, 22].

Figures 6 and 7 show the effect of clay content on the nanomorphology of the samples. XRD results indicate that there is an increase in orientation of the layered silicate as the clay content was increased. A significant level of orientation is shown at 10% loading, especially using FLUKA in RPET and VPET (Figures 6a and 7b). However, for VPET-PHIL samples (Figure 7a), no significant intensity peaks at the low-angle basal (001) reflections in various clay loadings were observed. The absence of basal plane peaks indicates the delamination and dispersion of OMMT (PHIL) nanolayers within the polymer matrix thus, allowing the formation of an exfoliated nanostructure [23]. Figure 8 indicates that RPET-PHIL and VPET-PHIL systems, both with 5% clay content, exhibited similar crystallographic structure despite the difference of the thermal and mechanical history before melt intercalation of the two resins.

SAXS results show that there is a broadening of intensity peak at around 0.5 ( $2\theta$ ) for system VPET-FLUKA (5%) in Figure 9. The same behavior was observed (Figure 10) for RPET-PHIL system at various clay loadings, giving a d-spacing of 14nm at basal (001) reflections. This revealed the existence of partially laminated structures that were not observed in XRD.

XRD is useful for the measurement of d-spacings in intercalated systems but cannot always be observed at low clay loadings (<5%) or be used as a method to identify an exfoliated nanocomposite where no XRD peaks are present [24]. The overall nanoscale dispersion of the organo-modified montmorillonite in the PET matrix is best observed by TEM analysis. Figure 11(A) shows generally exfoliated structures in the PET matrix. At higher magnification, the presence of laminated (B) and exfoliated structures (C) was observed. These results are in agreement with the SAXS data. Moreover, higher clay loadings cause the samples to be agglomerated or not fully dispersed uniformly in the matrix as shown in the TEM micrographs of Figure 12. Practically, it is difficult to get fully exfoliated (or fully intercalated) polymer/clay nanocomposites at higher clay loadings, especially by melt intercalation approach [25].

### 3.3.2 *Thermal stability and mechanical properties of polymer nanocomposites*

Results of DSC (Figure 13 and Table 1) show that there is no significant difference in thermal properties of using organoclays: FLUKA and PHIL in RPET nanocomposites. However, intercalating VPET in FLUKA and PHIL showed a lower Tg. This is because the Tg of the neat PET resin is lower than RPET before the melt intercalation process. Moreover, there was a decrease in Tg as the clay content was increased (Figure 14 and Table 1). The Tm remained almost the same in all the mixtures, however, at 10% loading a completely amorphous structure was obtained. All the samples showed cold crystallizations.

The PHIL organoclay showed good thermal stability, while the nanocomposite samples degraded abruptly at 450<sup>0</sup>C (Figure 15). The molecular structure of the quaternary alkylammonium ion is also the determining factor of the thermal stability of nanocomposites. The thermal stability is also related to the OMMT content and the dispersion of the clay in the PET matrix [26,27]. Since there is only inorganic aluminosilicate left in the system at that stage, it is not surprising that the nanocomposites show slower degradation above 450<sup>0</sup>C. Adding organoclays enhances the thermal stability of nanocomposite. Pramoda, et. al [28] added that only exfoliated polymer nanocomposites exhibit improved thermal stability. In this study, a mixture of exfoliated and laminated structures exhibited good thermal stability at higher clay loadings. Generally, the RPET-PHIL exhibited thermal properties similar to that of the VPET-PHIL (Figure 16).

The mechanical behavior of the nanocomposites at various clay loadings (Figure 17) shows that the higher the clay content the better is the tensile strength of the samples. Ten (10) percent clay loading in the matrix enhanced the strength by about 75% compared to the neat resin. However at 10% clay content a slight decrease of modulus was observed. This maybe due to the agglomeration or incomplete dispersion of the montmorillonite particles in the PET matrix as seen in the TEM micrographs.

## **IV. Conclusions**

Organic-activation of Philippine montmorillonite with alkyl ammonium cations created lamellar, multi-layered expanded structures exposing it for intercalation with polymers.

Direct melt intercalation by extrusion gave a generally exfoliated structure at ≤5% clay loadings using Philippine organo-modified montmorillonite in RPET matrix. However, at very low angle, localized laminated structures were determined by SAXS and supported by TEM.

Philippine organo-montmorillonite intercalated with VPET resin exhibited exfoliated structures even at higher clay loadings (10%), revealing good miscibility of this organic-inorganic hybrid.

The thermal stability of the RPET/organo-montmorillonite nanocomposites has been enhanced and the tensile strength improved with the increase in organoclay loading.

In general, favorable enthalpy of mixing for the PET (recycled or neat resin) and the organically modified montmorillonite was achieved. The PET was confined in the interlayer spaces producing generally exfoliated structures and mixed nanomorphologies in some systems, using the direct melt intercalation method.

## V. Acknowledgements

This research was made possible by the following: Japan Society for the promotion of Science (JSPS), Institute of Multidisciplinary Research for Advance Materials (IMRAM) of Tohoku University, Institute of Materials Research and Engineering (IMRE) – Singapore, Department of Science and Technology-Philippines, and the Office of the Vice-Chancellor for Research and Development (OVCRD)-University of the Philippines.

## References

1. Gilman, J.W., Jackson, C.L., Morgan, A.B. and Harris, Jr., R., "Flammability Properties of Polymer-Layered-Silicate Nanocomposites: Polypropylene and Polystyrene Nanocomposites", *Chemistry of Materials*, **12**, 1866-1873 (2000).
2. Dagani, R., "Putting the 'Nano' into Composites", *Science/Technology CENEAR 77*, **77** [23] 25-37 (1999).
3. Kamena, K., "An Emerging Family of Nanomer Nanoclays for the Plastics Industry", *Nanocor Report*, Nanocor Inc. , USA (1999).
4. Galgali, G., Lee, A. and Ramesh, C., "Rheological Study on the Kinetics of Hybrid Formation in Polypropylene Nanocomposites", *Macromolecules*, **34** [4] 852-858 (2001).
5. Degaspari, J., "Eye on the Future: Nanotechnology", *Mechanical Engineering Magazine*, **1**, 1-6(2002).
6. Duquet, E. *University Bordeaux-1 Research Report*, Germany (2000).
7. Manias, E., Jackson, C.L., Morgan, A.B. and Harris Jr., R., "Clay Fillers Point Way to Reducing Flammability in Many Polymers", *American Chemical Society Publications*, USA (2000).
8. EREMA, *PET Recycling with Patented Erema Technology*, EREMA Plastics Recycling Systems, Austria (2002).
9. Basilia, B. and Prokopovich, S., "Synthesis and Characterization of Bentonites of Different Organophilicities", *Proceedings of the 2<sup>nd</sup> International Meeting of PACIFIC RIM CERAMIC SOCIETIES – PACRIM 2*, Cairns, Australia (1996).
10. Basilia, B. and Prokopovich, S., "Synthesis of Philippine Organophilic Bentonite for the Surface Coating Industry", *Proceedings of the 9<sup>th</sup> Asia Pacific Coating Conference*, Manila, Philippines (1999).
11. Favre, H. and Lagaly, G., "Organo-bentonites with Quaternary Alkylammonium Ions", *Clay Minerals*, **26** [1] 19-32 (1992).
12. Theng, B.K.G., *The Chemistry of Clay-Organic Reactions*, Wiley, New York, USA (1974).
13. Sichina, W.J., "DSC as Problem Solving Tool: Measurement of Percent Crystallinity of Thermoplastics", *Thermal Analysis Application Note*, Perkin Elmer Instruments, USA (2002).
14. ASTM D 638-91 "Standard Test Methods for Tensile Properties of Plastics" (1991).



15. Lagaly, G., Gonzalez, M.F. and Weiss, A., "Problems in Layer-Charge Determination of Montmorillonites", *Clay Minerals*, **11**, 173-187 (1976).
16. Bujdak, J. and Slosiarikova, J., "The Reaction of Montmorillonite with Octadecylamine in Solid and Melted State", *Applied Clay Science*, **7**, 263-269 (1992).
17. Giannelis, E. P., Krishnamoorti, R. and Manias, "Polymer-silicate Nanocomposites: Model System for Confined Polymers and Polymer Brushes", *Advances in Polymer Science*, **138**, 107-147 (1999).
18. Fu, X. and Qutubuddin, S., "Nanocomposites: Exfoliation of Organophilic Montmorillonite Nanolayers in Polystyrene", *Polymer*, **42**, 807-813 (2001).
19. Sichina, W.J., "Isothermal Crystallization of Polymers", *Thermal Analysis Application Note*, Perkin Elmer Instruments, USA (2002).
20. Bielefeld, M.Z. and Schwerzenback, G.W., "Thermoplastics", *Collected Applications: Thermal Analysis*, Mettler Toledo, Switzerland (1997).
21. Bharadwaj, R.K., Mehrabi, A.R., Hamilton, C., Trujillo, C., Murga, M., Fan, R., Chavira, A. and Thompson, A.K., "Structure-Property Relationships in Cross-Linked Polyester-Clay Nanocomposites", *Polymer*, **43**, 3699-3705 (2002).
22. Strawhecker, K.E. and Manias, E., "Structure and Properties of Poly(vinyl alcohol)/Na<sup>+</sup> Montmorillonite Nanocomposites", *Chemistry of Materials*, **12**, 2943-2949 (2000).
23. Pramoda, K.P., Liu, T., Liu, Z., He, C. and Sue, H., "Thermal Degradation Behavior of Polyamide 6/Clay Nanocomposites", *Polymer Degradation and Stability*, **81**, 47-56 (2003).
24. Morgan, A.B. and Gilman, J.W., "Characterization of Polymer-Layered Silicate (Clay) Nanocomposites by Transmission Electron Microscopy and X-ray Diffraction: A Comparative Study", *Journal of Applied Polymer Science*, **87**, 1329-1338 (2003).
25. Liu, T.X., Liu, Z.H., Ma, K.X., Shen, L., Zeng, K.Y. and He, C.B., "Morphology, Thermal and Mechanical Behavior of Polyamide 6/Layered-silicate Nanocomposites", *Composites Science and Technology*, **63**, 331-337 (2003).
26. S. Wang, Y. Hu, Z. Wang, T. Yong, Z. Chen and W. Fan, "Synthesis and Characterization of Polycarbonate/ABS/montmorillonite Nanocomposites", *Polymer Degradation and Stability*, **80**, 157-161 (2003).
27. C. F. Ou, M. T. Ho and J.R. Lin, "Synthesis and Characterization of Poly(ethylene terephthalate) Nanocomposites with Organoclay", *Journal of Applied Polymer Science*, **91**, 140-145 (2004).
28. Pramoda, K.P., Liu, T., Liu, Z., He, C. and Sue, H., "Thermal Degradation Behavior of Polyamide 6/Clay Nanocomposites", *Polymer Degradation and Stability*, **81**, 47-56 (2003).

## Figures

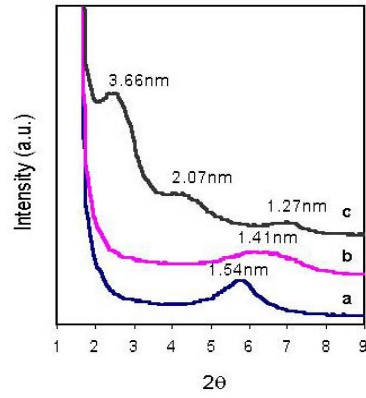


**Figure 1.** XRD spectra of Philippine montmorillonite: a) Ca-MMT, b) Na-MMT, and c) OMMT.

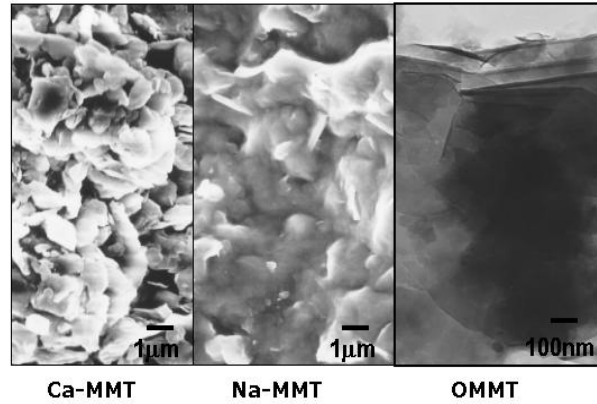


**Figure 2 .** Micrographs of Philippine montmorillonites: FESEM of Ca-MMT and Na-MMT, and TEM of OMMT.

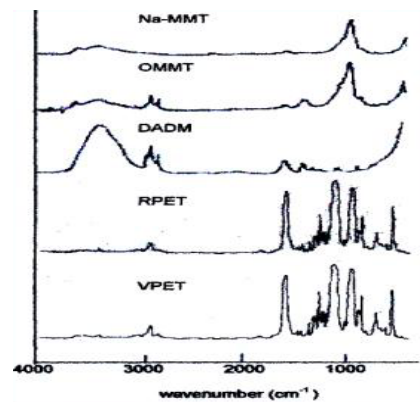


**Figure 3 .** FTIR spectra of montmorillonites and PET resins.

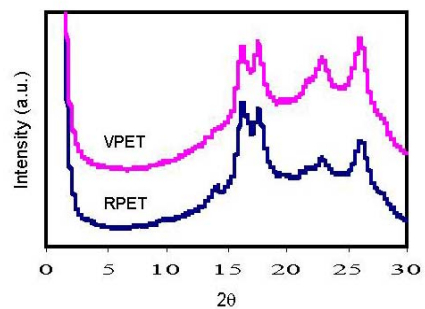


Figure 4. XRD spectra of VPET and RPET resins.

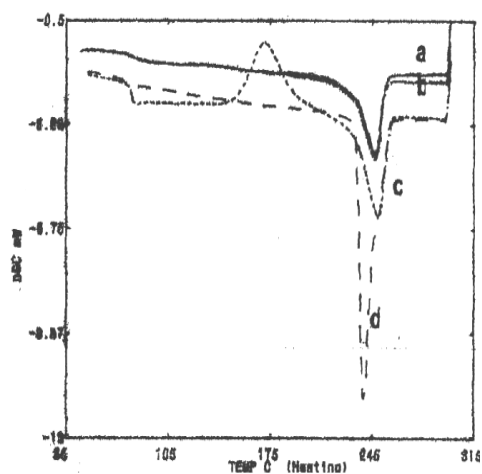


Figure 5. DSC of RPET [1<sup>st</sup> htg (a) and 2<sup>nd</sup> htg (b)], and VPET [1<sup>st</sup> htg (c) and 2<sup>nd</sup> htg (d)].

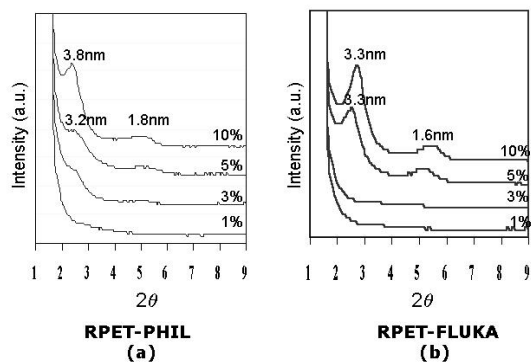
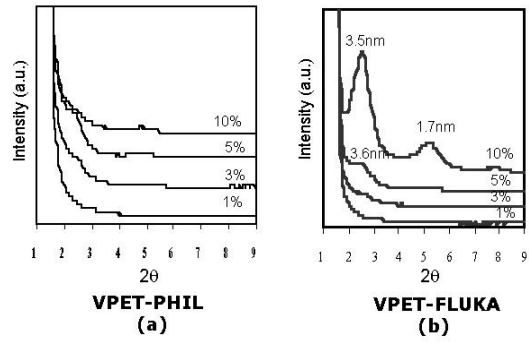
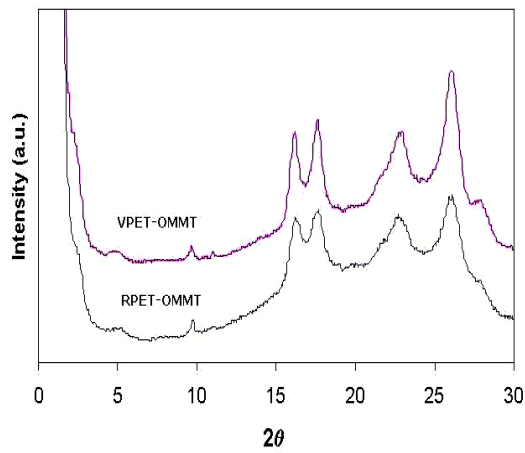


Figure 6. XRD spectra of RPET-PHIL and RPET-FLUKA at various clay loading.



**Figure 7.** XRD spectra of VPET-PHIL and VPET-FLUKA at various clay content.



**Figure 8.** XRD of RPET-OMMT and VPET-OMMT systems.

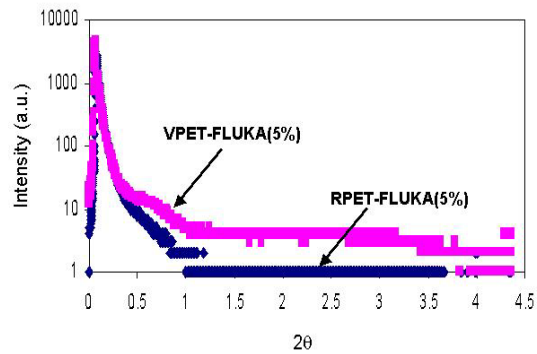


**Figure 9.** SAXS patterns of VPET and RPET with FLUKA.

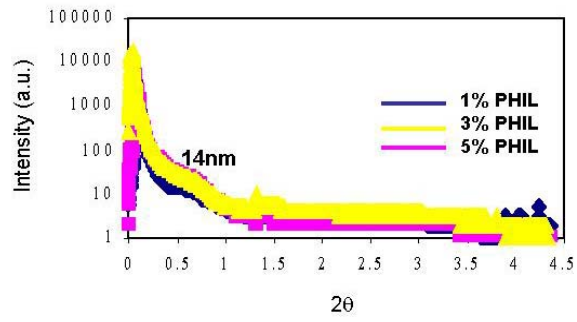


**Figure 10.** SAXS patterns of RPET-PHIL system at various clay loading.

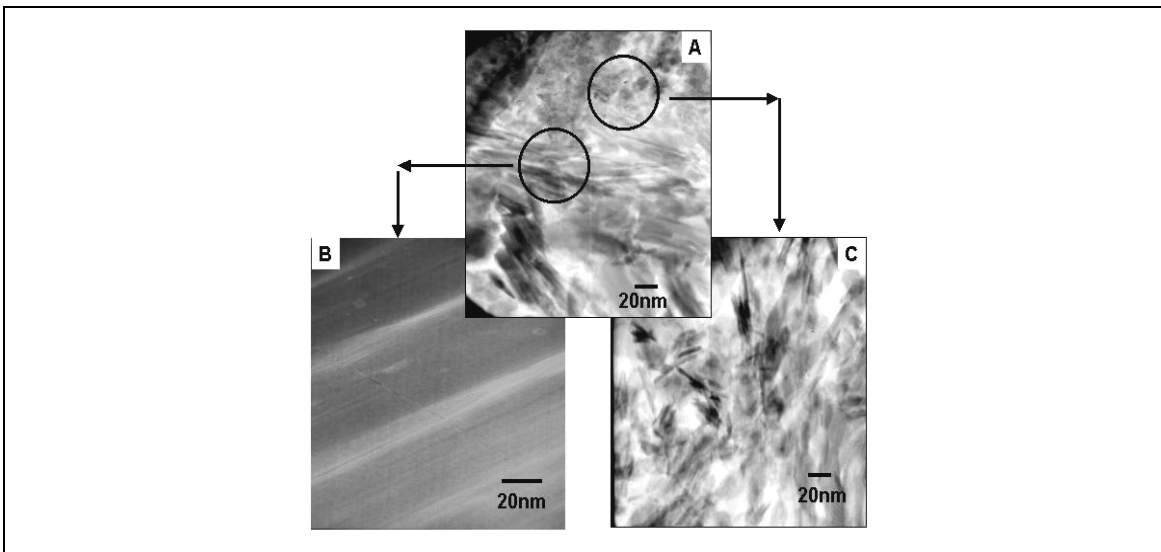


**Figure 11.** TEM of RPET-PHIL system.

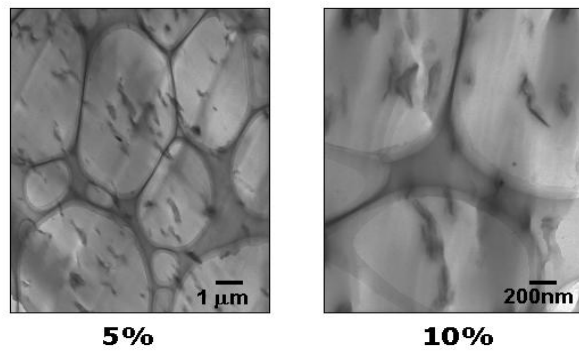


**Figure 12.** TEM of RPET-PHIL SYSTEM at 5% and 10% clay loading.

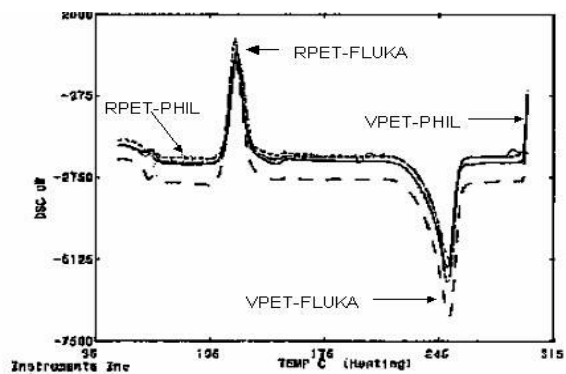


Figure 13. DSC of RPET and VPET with FLUKA and PHIL at 5% clay content.

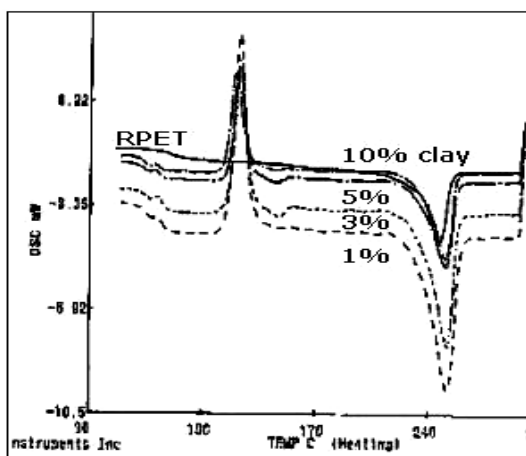


Figure 14. DSC of RPET-PHIL system at various clay loading.

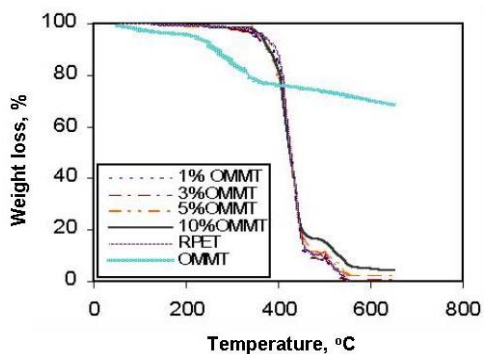
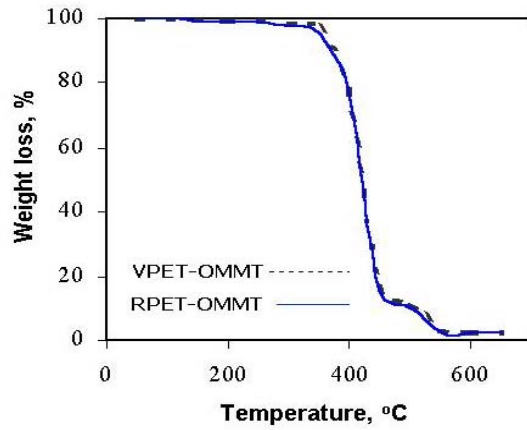
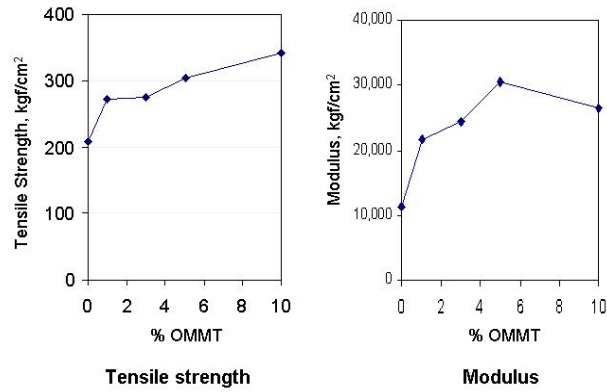


Figure 15. TGA of RPET-PHIL system at various clay loading.



**Figure 16.** TGA of RPET-OMMT and VPET-OMMT systems.



**Figure 17.** Mechanical properties of RPET-PHIL (OMMT) system at various clay loading.

**Table 1**  
Summary of DSC data.

<b>SAMPLE</b>	<b>Tg (°C)</b>	<b>Tc (°C)</b>	<b>Tm (°C)</b>	<b>Hc (J/g)</b>	<b>Hm (J/g)</b>	<b>%C</b>
<b>Resins:</b>						
RPET-1 <sup>st</sup> htg	83.4		247.5		23.6	20.5
2 <sup>nd</sup> htg	85.8		246.8		23.5	20.4
VPET-1 <sup>st</sup> htg	76.2		239.9		36.7	31.91
2 <sup>nd</sup> htg	80.3	171.6	249.2	20.8	21.1	0.3
<b>% Loading:</b>						
1% OMMT	75.0	122.7	251.7	19.0	26.5	6.5
3% OMMT	75.0	122.8	251.4	18.8	27.4	7.5
5% OMMT	73.3	120.2	251.1	19.8	28.0	7.2
10% OMMT	72.4	122.1	251.1	25.0	25.4	0.3
<b>Nanocomposite:</b>						
RPET-FLUKA	72.5	121.5	250.6	17.9	25.2	6.3
RPET-PHIL	72.4	120.2	251.1	19.8	28.0	7.2
VPET-FLUKA	65.1	120.2	251.1	18.2	26.5	7.2
VPET-PHIL	70.5	121.5	251.1	19.9	28.8	7.7